

M3D III:

Mechanics and Mechanisms of Material Damping

*Alan Wolfenden
Vikram K. Kinra*

EDITORS



STP 1304

STP 1304

M³D III: Mechanics and Mechanisms of Material Damping

Alan Wolfenden and Vikram K. Kinra, editors

ASTM Publication Code Number (PCN):
04-013040-23



ASTM
100 Barr Harbor Drive
West Conshohocken, PA 19428-2959

Printed in the U.S.A.

Library of Congress Cataloging-in-Publication Data

M³D III : mechanics and mechanisms of material damping / Alan Wolfenden and Vikram K. Kinra, editors.

p. cm. — (STP ; 1304)

"International Symposium on "M³D III: Mechanics and Mechanisms of Material Damping" took place in Norfolk, Virginia, 15-17 Nov. 1995

... sponsored by ASTM Committee E28 on Mechanical Testing in cooperation with the U.S. Office of Naval Research"—

Includes bibliographical references and index.

ISBN 0-8031-2417-1

1. Damping (Mechanics)—Congresses. 2. Material—Mechanical properties—Congresses. 3. Internal friction—Congresses.

I. Wolfenden, Alan, 1940-

II. Kinra, Vikram K., 1946-

III. American Society for Testing and Materials. Committee E-28 on Mechanical Testing. IV. United States. Office of Naval Research.

V. International Symposium on "M³D: Mechanics and Mechanisms of Material Damping" (3rd : 1995 : Norfolk, Va.) VI. Series: ASTM special technical publication ; 1304.

TA418.32.M2 1997

620.3—dc21

97-36338

CIP

Copyright© 1997 AMERICAN SOCIETY FOR TESTING AND MATERIALS, West Conshohocken, PA. All rights reserved. This material may not be reproduced or copied, in whole or in part, in any printed, mechanical, electronic, film, or other distribution and storage media, without the written consent of the publisher.

Photocopy Rights

Authorization to photocopy items for internal, personal, or educational classroom use, or the internal, personal, or educational classroom use of specific clients, is granted by the American Society for Testing and Materials (ASTM) provided that the appropriate fee is paid to the Copyright Clearance Center, 222 Rosewood Drive, Danvers, MA 01923; Tel: 508-750-8400; online: <http://www.copyright.com/>.

Peer Review Policy

Each paper published in this volume was evaluated by two peer reviewers and at least one of the editors. The authors addressed all of the reviewers' comments to the satisfaction of both the technical editor(s) and the ASTM Committee on Publications.

The quality of the papers in this publication reflects not only the obvious efforts of the authors and the technical editor(s), but also the work of these peer reviewers. The ASTM Committee on Publications acknowledges with appreciation their dedication and contribution to time and effort on behalf of ASTM.

Foreword

The international symposium on M³D III: Mechanics and Mechanisms of Material Damping was presented in Norfolk, Virginia, 15–17 Nov. 1995. The symposium was sponsored by ASTM Committee E28 on Mechanical Testing in cooperation with the U.S. Office of Naval Research. Alan Wolfenden and Vikram K. Kinra of Texas A&M University, Rene De Batist of the University of Antwerp, Belgium, Larry Kabacoff of the Office of Naval Research, Arlington, and Cathy Wong of the Naval Surface Warfare Center, Annapolis, presided as chairpersons of the symposium. The editors of this publication are Alan Wolfenden and Vikram K. Kinra.

Contents

Overview	1
High-Temperature Internal Friction and Intergranular Fracture in Ni-Cr Alloys —B. CAO, W. BENOIT, AND R. SCHALLER	4
Dislocation Amplitude-Dependent Damping in Crystals —S. B. KUSTOV AND S. N. GOLYANDIN	22
A Study of the Internal Friction Associated with Discontinuous Precipitation in Lead-Tin Alloys —J. LU, D. C. VAN AKEN, AND H. P. LEIGHLY, JR.	46
Composite Rotorcraft Flexbeams with Viscoelastic Damping Layers for Aeromechanical Stability Augmentation —C. B. SMITH AND N. M. WERELEY	62
Modeling Dislocation Breakaway Damping and Harmonic Generation —D. N. BESHES	78
Mechanical Damping in the Martensitic Phase of Cu-Al-Ni Crystals —S. B. KUSTOV, J. VAN HUMBEECK, I. HURTADO, S. N. GOLYANDIN, AND R. DE BATIST	94
Magnetomechanical Damping in Thermally Sprayed Fe-Cr-X Coatings —A. KARIMI, P. H. GIAUQUE, AND J. L. MARTIN	115
Damping Due to Grain Boundary Sliding in Zirconia and Alumina —A. LAKKI AND R. SCHALLER	128
Investigation of the High-Temperature Damping of the Nickel-Base Superalloy CMSX-4 in the kHz-Range —W. HERMANN AND H.-G. SOCKEL	143
Magnetoplastic Effect: Relaxation of the Dislocation Structure and Microcreep of Nonmagnetic Crystals —V. I. ALSHITS, E. V. DARINSKAYA, O. L. KAZAKOVA, E. Y. MIKHINA, AND E. A. PETRZHIK	153
Effect of Crystalline and Magnetic Structure on Magnetomechanical Damping of Fe-Cr-Based Alloys —I. B. CHUDAKOV AND I. S. GOLOVIN	162
Internal Friction Spectrum Analysis for Complex Alloyed Austenitic Steels —I. S. GOLOVIN, R. V. ZHARKOV, AND S. A. GOLOVIN	179
Critical Experimental Data on the Snoek-Köster Relaxation and Their Explanation by the Coupling Model —L. B. MAGALAS AND K. L. NGAI	189
Mechanism for the High Damping State in Alloys of the Fe-Al System —V. A. UDOVENKO, I. B. CHUDAKOV, AND N. A. POLYAKOVA	204
Comparison of Elastic and Anelastic Properties of SiC and MoSi₂/Ti₅Si₃ as a Function of Temperature —A. WOLFENDEN, K. J. BAUER, P. B. KURY, K. A. OLIVER, P. J. RYNN, J. J. PETROVIC, AND M. SINGH	214

Young's Modulus and Mechanical Loss in PZT Ceramics Associated with Phase Transitions —B. L. CHENG, M. GABBAY, AND G. FANTOZZI	227
An Experimental Comparison of the In-Air and Underwater Damping Properties of Composite Cylinders —R. M. CRANE AND C. P. RATCLIFFE	239
Amplitude-Dependent Damping in YBCO Ceramics Between 6.5 K and 290 K —B. K. KARDASHEV, S. N. GOLYANDIN, S. B. KUSTOV, S. P. NIKANOROV, P. DEVOS, J. CORNELIS, AND R. DE BATIST	251
Anelasticity of Single and Polycrystalline Materials by the Resonant Sphere Technique (RST) —I. SUZUKI	267
Snoek Relaxation in Fe-Cr Alloys (0 to 100% Cr) —I. S. GOLOVIN, M. S. BLANTER, A. MOURISCO, AND R. SCHALLER	278
Factors Affecting the Damping Capacity of TiC Particle Reinforced Zinc-22 Aluminum Composites —J. LU AND D. C. VAN AKEN	288
Amplitude-Dependent Material Damping—Old Beliefs and New Facts: Working Toward a Synthesizing Model —D. GELLI AND E. OLZI	302
Damping Behavior of 6061Al/SiC/Gr Spray-Deposited Composites —J. ZHANG, R. J. PEREZ, AND E. J. LAVERNIA	313
Modeling the Damping Mechanism in Electrorheological Fluid Based Dampers —G. M. KAMATH AND N. M. WERELEY	331
Probabilistic Technique Related to Amplitude-Dependent Damping Under Combined Stresses —S. G. CUPSCHALK	349
A Review of the Physical Metallurgy and Damping Characteristics of High Damping Cu-Mn Alloys —S. LADDHA AND D. C. VAN AKEN	365
Snoek Relaxation in Ternary Body-Centered-Cubic Alloys —H. NUMAKURA AND M. KOIWA	383
Computer Model of Zener Relaxation —M. S. BLANTER AND E. V. KOLESNIKOV	394
Author Index	407
Subject Index	409

Overview

The International Symposium on "M³D III: Mechanics and Mechanisms of Material Damping" took place in Norfolk, Virginia, 15–17 Nov. 1995. The Symposium was sponsored by ASTM Committee E28 on Mechanical Testing in cooperation with the U.S. Office of Naval Research. The Symposium was the third of a series: "M³D: Mechanics and Mechanisms of Material Damping" took place in Baltimore on 13–15 March 1991 and is documented in ASTM STP 1169; "M³D II: Mechanics and Mechanisms of Material Damping II" was convened in Pittsburgh on 18–21 Oct. 1993, was sponsored by TMS, The Metallurgical Society of AIME, and the U.S. Office of Naval Research, and is published in a special issue of Metallurgical Transactions, November 1995. At this third symposium, more than 48 colleagues representing ten countries, including the Former Soviet Union, participated. The main aim of the Symposium was to foster a synergistic interaction among researchers in the fields of mechanics of solids and materials science, with the added aim of spawning increased collaboration between the two fields of research.

Within the 48 h duration of the Symposium, four technical sessions and a panel discussion took place. Each session was chaired by two specially invited colleagues and started with a keynote address by an internationally recognized authority in a particular aspect of damping. Several contributed talks followed the keynote address. The Session Chairmen encouraged questions and discussion as an integral part of each talk. The Panel Discussion, moderated by a Symposium Chairman and having four carefully selected colleagues of international repute as Panel Members, formed the closing stage of the Symposium. This Discussion allowed the participants and Panel Members to follow up questions with mechanisms of material damping, and to sense the future directions of research on damping.

As the documented record of the International Symposium on M³D III, we have produced this Special Technical Publication (STP). It contains 28 papers which cover various aspects of damping, embracing both fundamental research and technological applications. Four keynote speakers led off the sessions of the Symposium and strove to emphasize the complementary roles of mechanics and materials in our understanding of material damping. The international interest in damping can be gaged from the fact that participants at the Symposium came from ten countries (Belgium, France, Germany, Italy, Japan, People's Republic of China, Poland, Russia, Switzerland, and the United States of America). Many of the papers have a natural bias toward either mechanics or materials, but some papers indicate the necessity of merging these disciplines to gain an enhanced understanding of damping.

The STP contains a wide range of topics relating mechanics, materials, and damping. This is because damping is a complex phenomenon. The topics covered include: nonlinear effects of boundaries, viscoelastic damping, grain boundary damping, high temperature damping, ceramics, superconductors, Snoek relaxation, high damping materials, composites, phase changes (both martensitic and solid-liquid), magnetomechanical damping, elastothermodynamic damping, Zener relaxation, layered and intercalated materials, electrorheological damping, modeling, longitudinal and flexural vibrations, and a host of specific materials.

The issue of accuracy in damping measurements was raised at the Panel Discussion. A future task is making available, for all the techniques of measuring damping, suitable standard reference materials with known values of damping.

Many people have helped the organizers of the Symposium. The Symposium Chairmen thank: the ASTM staff for their promotion of the Symposium and their guidance in the preparation of this STP; the Session Chairmen for their spirited control of the speakers and the discussions arising from the talks; the invited keynote speakers for bringing to the Symposium their knowledge on damping accumulated over many years; our colleagues from overseas for making the Symposium truly international; the anonymous reviewers for their time and comments for improving the manuscripts (in keeping with ASTM policy, each manuscript was reviewed by three reviewers); our colleagues in Committee E28 for their encouragement to hold the Symposium; and the U.S. Office of Naval Research, represented by Dr. L. Kabacoff, for its interest in the Symposium.

Alan Wolfenden

Mechanical Engineering Department,
Texas A&M University,
College Station, TX 77843;
symposium chairman and editor.

Vikram K. Kinra

Aerospace Engineering Department,
Texas A&M University,
College Station, TX 77843;
symposium chairman and editor.

Relationship Amongst Various Measures of Damping

(valid for small values of damping: $\tan \phi < 0.1$)

$$Q^{-1} = \frac{\Psi}{2\pi} = \eta = \frac{\delta}{\pi} = \tan \phi = \phi = \frac{E''}{E'} = 2\zeta = \frac{\Delta W}{2\pi W} = \frac{\lambda \alpha}{\pi}$$

Q = Quality Factor

Ψ = Specific Damping Capacity

η = Loss Factor

δ = Logarithmic Decrement

ϕ = Phase Angle by which Stress Leads Strain

E'' = Loss Modulus

E' = Storage Modulus

ζ = Damping Ratio or Damping Factor

ΔW = Energy Loss Per Cycle

W = Maximum Elastic Stored Energy

λ = Wavelength of Elastic Wave

α = Attenuation

High-Temperature Internal Friction and Intergranular Fracture in Ni-Cr Alloys

REFERENCE: Cao, B., Benoit, W., and Schaller, R., "High-Temperature Internal Friction and Intergranular Fracture in Ni-Cr Alloys," *M³D III: Mechanics and Mechanisms of Material Damping*, ASTM STP 1304, A. Wolfenden and V. K. Kinra, Eds., American Society for Testing and Materials, 1997, pp. 4–21.

ABSTRACT: Internal friction measurements have been performed on various compositions of polycrystalline alloys (Ni-8.6, 20 and 31.4 at.%Cr) and single crystals (Ni-20 and 33.6 at.%Cr), as well as in industrial alloys of Ni-22 at.%Cr containing respectively 0, 20, 66, and 180 at. ppm cerium.

The high-temperature internal friction spectra obtained in these alloys are characterized by the presence of two relaxation peaks (P1 and P2) and a large thermal hysteresis between the curves measured during heating and cooling. The P1 peak appears at about 950 K both in polycrystalline specimens and in single crystals. The P2 peak, appearing at about 1100 K, and the large thermal hysteresis occur only in the polycrystalline specimens. It is shown that the origin of P1 peak lies in the interior of the grains and that the P2 peak and the hysteresis are due to the grain boundaries. The P1 peak could be interpreted as a Zener peak due to local stress-induced ordering. The P2 peak is certainly due to grain boundary sliding, more precisely to grain boundary dislocation motion. These dislocations interact with chromium carbide precipitates located in the grain boundary. The hysteresis is then interpreted as due to the dissolution during heating and the reprecipitation upon cooling of these discrete carbides in the grain boundaries.

The three anelastic phenomena, the P1 and P2 peaks and the hysteresis, appear in the same temperature range where intergranular embrittlement was observed during tension tests. This embrittlement, as well as the P2 peak, is associated with grain boundary sliding and is enhanced by carbide dissolution. On the contrary, pinning of the grain boundaries by carbides leads to the disappearance of P2, and plastic deformation is then intragranular. It is shown that cerium additions stabilize the carbides at the grain boundaries. The penetration of oxygen along the grain boundaries, on the contrary, destabilizes the carbide precipitates and enhances grain boundary sliding.

KEYWORDS: internal friction, nickel-chromium alloys, intergranular embrittlement, Zener peak, grain-boundary peak, cerium, carbides, oxygen

The high-temperature deformation and fracture behavior of polycrystalline materials are strongly affected by the presence of both grain boundaries and impurities. The intergranular creep rupture phenomenon often occurs through formation, growth, and interlinkage of micro-cracks and cavities on the grain boundaries [1,2]. It is generally believed that grain boundary sliding is an essential process which causes stress concentration, and hence cavity nucleation at grain boundary irregularities, such as ledges, second-phase particles and triple points [1–4]. Therefore, the study of the influence of the structure on the mobility of grain boundaries is of great importance for understanding the high-temperature behavior of materials. However,

¹Ph.D. student, professor, and senior researcher, respectively. Ecole Polytechnique Fédérale de Lausanne, Institut de Génie Atomique, CH-1015 Lausanne, Switzerland.

information on atomic-scale movements cannot normally be obtained from conventional grain boundary sliding studies but can be obtained from internal friction measurements [5].

Phenomenologically, grain boundaries slide in a viscous manner under a shear stress field. Grain boundary sliding at small distances manifests itself in anelastic deformation and then internal friction arises [6–9]. Such sliding leads to an apparently lower shear modulus of the polycrystal [6,7,10]. Since Kê's discovery of an internal-friction relaxation peak attributed to grain boundary sliding in polycrystalline aluminum [7], internal friction measurements have been applied to a wide range of materials to study the grain boundary properties [8,11]. However, further internal friction experiments have led to additional models for the basic mechanism of high-temperature relaxation such as grain-boundary migration [12], the movement grain boundary dislocations [13–15], and lattice dislocations [16]. At present, the detailed mechanism is not yet well known and even the controversy about the origin of the high-temperature relaxation is still not completely resolved [17,18].

Our previous results from internal friction measurements on commercial nickel-chromium-cerium alloys have revealed some anelastic phenomena which could be related to the grain boundaries [19–22]. In the present work, the high-temperature elastic and anelastic behaviors are systematically investigated on various compositions of polycrystalline and single crystals of pure nickel-chromium alloys. In parallel with the internal friction measurements, conventional and in situ heating transmission electron micrograph (TEM) observations have been carried out on the measured specimens in order to correlate the microstructural state, especially at grain boundaries, with the corresponding internal friction spectra. Relaxation mechanisms are discussed as well as the relation between these mechanisms and the presence or absence of intergranular embrittlement.

Experimental Method

Materials

The alloys used for this work were prepared with high-purity nickel (99.99%) and chromium (99.996%) by the Institute of Applied Physics, Swiss Federal Institute of Technology Zurich (ETHZ). Polycrystalline alloys with nominal compositions of Ni-20 and 33 at.%Cr were fabricated by vacuum induction melting followed by casting. The alloy with the nominal composition of Ni-10 at.%Cr was obtained through the dilution of a Ni-33 at.%Cr alloy by adding an adequate quantity of pure nickel. Single-crystal alloys with nominal compositions of 22 and 33 at.%Cr were grown by the Bridgman technique in an alumina crucible. The chemical compositions of the alloys which were used are listed in Table 1.

The specimens for the internal friction measurements were spark-machined in the form of thin bars $60 \times 2.5 \times 0.5 \text{ mm}^3$ (for the low-frequency torsion pendulum) and $60 \times 1 \times 4 \text{ mm}^3$ (for the forced-inverted torsion pendulum). Before measuring, all of the polycrystalline specimens were vacuum annealed for 10 min at 1323 K to obtain a similar grain size of about

TABLE 1—Typical chemical compositions of Ni-Cr alloys used for present work (at.%).

Alloy Types	Nominal Compositions (at.%)	Ni	Cr	C
Polycrystals	Ni-10Cr	Balance	8.6	0.02687
	Ni-20Cr	...	19.6	0.01466
	Ni-33Cr	...	31.4	0.04397
Single crystals	Ni-20Cr	...	19.6	0.00977
	Ni-33Cr	...	33.6	0.02687

80 μm and then aged under vacuum for 24 h at 1200 K to stabilize the microstructure. That the specimens were monocrystalline was verified by Laue X-ray analysis after electrolytic etching, and then they were annealed at 1200 K for several hours before the measurement to eliminate any possible handling effects.

Internal Friction Measurements

Internal friction and dynamic shear modulus measurements were performed mainly on a low-frequency torsion pendulum [23]. Measurements were carried out during heating and cooling at a rate of 2 K/min. The strain amplitude during the measurements was less than 3×10^{-5} . The whole apparatus was held under a vacuum better than 5×10^{-5} Torr. The data were acquired through a Hewlett Packard (HP) Data Acquisition and Control Unit and processed by a HP microcomputer. The internal friction values were deduced from the free-decay signal by means of a Fast Fourier Transformation [24]. Since the dynamic shear modulus G is proportional to the square of the vibration frequency, the normalized elastic shear modulus $G/G_{300\text{K}}$ was directly obtained from the frequency measurement.

Some internal friction and dynamic shear modulus measurements were also performed in an inverted torsion pendulum working with forced vibrations [25]. In this apparatus, the system is torsionally excited at an imposed frequency and the specimen deformation is detected by optical cells, whose amplified signals are processed by a signal analyzer. Internal friction Q^{-1} and the normalized elastic shear modulus $G/G_{300\text{K}}$ can be determined directly by measuring the phase lag between applied stress and resulting strain ϕ and the ratio of their amplitudes. It can be shown that, as a good approximation, $Q^{-1} = \tan \phi$ [8]. The temperature range of the apparatus can vary from room temperature to 1660 K and the applied frequency range between 10^{-4} and 10 Hz. The internal friction Q^{-1} and dynamic shear modulus $G/G_{300\text{K}}$ spectra can be acquired either as a function of temperature at fixed frequency or as a function of frequency at fixed temperature. The number of experimental points is high enough to obtain a continuous curve on the figures with sometimes a small dispersion (Fig. 1).

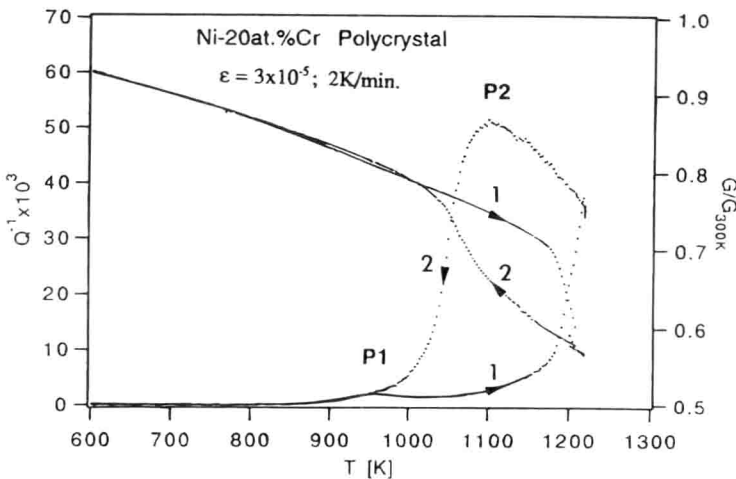


FIG. 1—Characteristic internal friction (Q^{-1}) and dynamic shear modulus (G) spectra of Ni-20Cr polycrystal, measured as a function of temperature upon heating (1) and cooling (2).

Experimental Results

Characteristic Spectra of Polycrystals

A typical result of internal friction and normalized elastic shear modulus as a function of temperature in polycrystalline Ni-20Cr, obtained both during heating and cooling, is shown in Fig. 1. This figure shows that the internal friction spectrum is characterized mainly by two internal friction peaks marked P1 and P2, respectively, as well as by a large thermal hysteresis between the curves obtained during heating and cooling. During heating, a small peak P1 (2×10^{-3}) superimposed on a high-temperature background, appears at about 950 K. A sharp increase in the internal friction background occurs between 1180 K and 1200 K, which is accompanied by a large drop in dynamic shear modulus. This is indicative of a softening of the alloy. Upon cooling, the background remains high and a new peak P2 is observed at about 1100 K. This peak is followed by a rapid decrease in internal friction around 1100 K, as well as by an increase of the shear modulus. This important evolution appears in the temperature range of the P1 peaks, and makes it difficult to recognize the presence of the P1 peak upon cooling.

Another experiment has been made with polycrystalline Ni-33Cr alloys and the result is shown in Fig. 2. It can be seen that the spectra of internal friction and elastic shear modulus as a function of temperature are essentially similar to those obtained in Ni-20Cr (Fig. 1). This suggests that the phenomena responsible for the observed elastic and anelastic behaviors at high temperature are of the same nature in these two compositions of polycrystalline Ni-Cr alloys. The temperatures of the P1 and P2 peaks, however, both shift to higher temperature with increasing chromium content and if the peak height of P1 peak increases, the peak height of P2 peak obviously decreases. In addition, the critical temperature corresponding to the sharp increase upon heating and the rapid decrease upon cooling in internal friction seem to appear at slightly higher temperature in the Ni-33Cr than in the Ni-20Cr specimen.

It should be pointed out that the spectra of internal friction and dynamic shear modulus evolution presented in Figs. 1 and 2 are completely reproducible during heating and cooling, under normal experimental conditions (that is, a vacuum better than 5×10^{-5} Torr). A

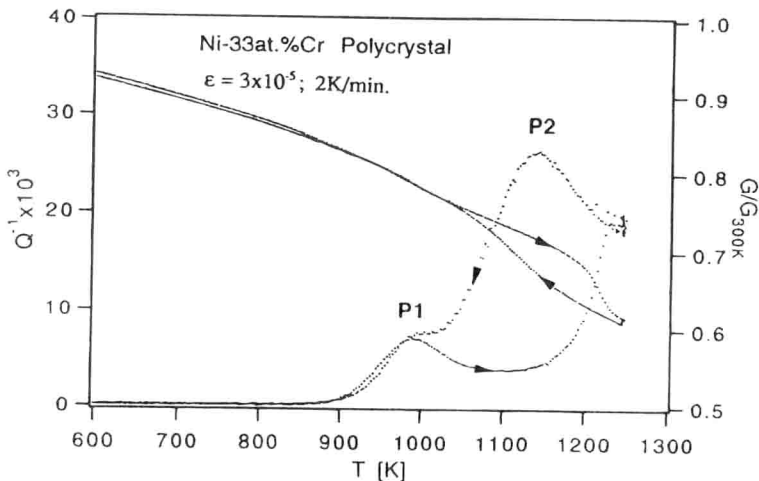


FIG. 2—Internal friction $Q^{-1}(T)$ and dynamic shear modulus $G(T)$ spectra of a polycrystalline Ni-33Cr specimen.

continuous evolution of the spectra was observed only in an oxygen-contaminated environment (cf. later subsection “Cerium and oxygen influence”).

Spectra of Single Crystals

In order to localize the origin of the above-mentioned anelastic phenomena, P1 and P2 peaks and the large thermal hysteresis, internal friction and shear modulus measurements have been performed also on Ni-20 and Ni-33Cr single-crystal specimens. In this case, only the P1 peak is observed at the same temperature and with a similar peak height as observed in the polycrystalline specimens during heating as well as during cooling (Fig. 3), whereas the P2 peak and the large thermal hysteresis are absent. As one can see from Fig. 3, the dynamic shear modulus of Ni-20Cr single crystals reduces to only about 0.70 of its value at room temperature at 1223 K. So, the polycrystalline specimens, in comparison with single crystals, show a lower dynamic shear modulus at high temperatures.

Because the grain boundaries are absent in the case of single crystals, it may be suggested that the origins of the P1 peak and the high-temperature background are within the grains. On the contrary, the P2 peak and the large thermal hysteresis, which appear only in polycrystals, may originate from the grain boundaries.

Evolution of the Spectra during the Recrystallization of a Single Crystal

High-temperature internal friction can also depend on the nature of the metal, on the purity and on the crystalline structure [26,27]. To be absolutely sure that the difference in the spectra between poly- and single crystals is related only to the presence or absence of grain boundaries, two special experiments were designed to observe the evolution of the internal friction spectra during the transition from single crystalline to polycrystalline state. The internal friction spectra and dynamic shear modulus spectra of Ni-20Cr single crystal were measured first (Fig. 4, curves 1, 2). The specimen was then cold-rolled at room temperature to a deformation of about 12% and measured again in the pendulum. The first heating after cold-rolling is shown by curve 3 in Fig. 4. After an annealing of 6 h at 1200 K to recrystallize and stabilize the

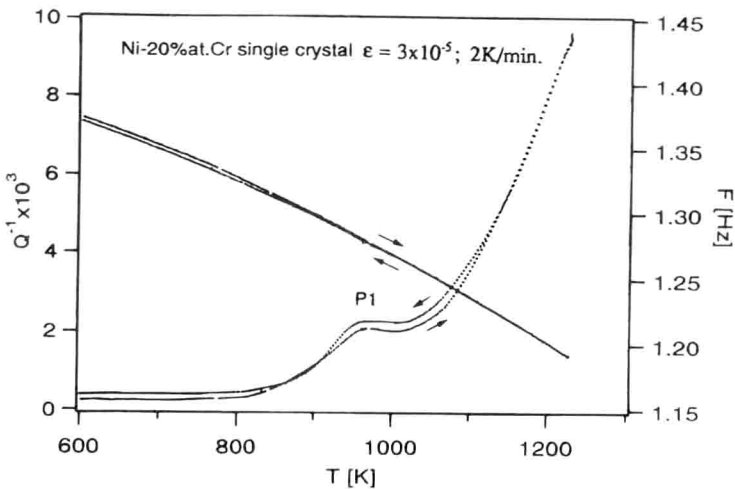


FIG. 3—Internal friction $Q^{-1}(T)$ and dynamic shear modulus $G(T)$ spectra of a single crystal of (1) Ni-20Cr.

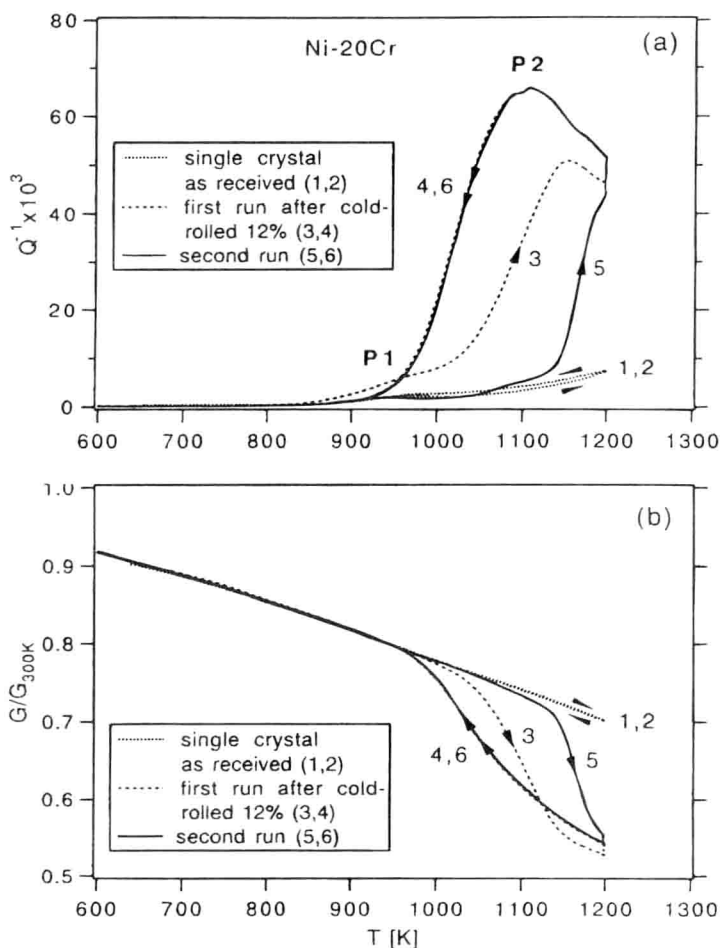


FIG. 4—Evolution of internal friction $Q^{-1}(T)$ and dynamic shear modulus $G(T)$ spectra of a Ni-20Cr single crystal. Curves 1 and 2 for initial state; curve 3, heating run after cold-rolling about 12% at room temperature; curve 4, cooling run after annealing of 6 h at 1200 K; curves 5 and 6, subsequent heating and cooling run.

structure, the P2 peak appears immediately upon cooling, with a significant recovery of the shear modulus (Fig. 4, curve 4). During the following thermal cycles, the spectra of internal friction and shear modulus, identical to that of polycrystalline specimen shown in Fig. 1, were observed (Fig. 4, curves 5, 6). The recrystallization was then believed to be completed during the annealing of 6 h at 1200 K mentioned before. In another experiment, the specimen was cold-rolled successively up to more than 12% and the internal friction measurements were performed after each cold-rolling. Then the evolution of the spectrum from that of a single crystal to a polycrystal was distinctively observed [23]. One notices also that once the recrystallization is completed, the spectra become stable and are almost not influenced by the subsequent deformation. Effectively, metallographical observations on these two specimens confirmed that the

recrystallization was taking place when the P2 peak was appearing, and showed also the presence of discrete carbide precipitates at the grain boundaries.

From this experimental evidence, it is then possible to conclude that the origin of the P2 peak and the large hysteresis really comes from the grain boundaries. On the contrary, the P1 peak is related to a mechanism which takes place in the interior of the grains.

Effect of Test Frequency

In order to investigate further the observed elastic and anelastic behavior in Ni-Cr alloys, the spectra of internal friction and dynamic shear modulus have been carried out with several test frequencies. It has been shown that the peak position of both P1 and P2 peaks shifts to higher temperature with increasing frequency [23,28]. This suggests that P1 and P2 are relaxation processes and that the mechanisms responsible for the peaks are thermally activated. However, the sharp increase and the rapid decrease in internal friction during the thermal cycling (thermal hysteresis) seem not to be sensitive to the changes in the frequency, as does the dynamic shear modulus. This is not indicative of thermally activated phenomena, but rather characteristic of structural evolution, such as phase transformation processes.

Discussion of Peak P1

Relaxation Parameters

To separate the P1 peak from the high-temperature background (which increases with the temperature), we have supposed that the mechanisms responsible for the P1 peak and the high-temperature background are independent and that the internal friction background evolves with the temperature following an exponential law

$$Q^{-1} = A \exp(-B/kT) \quad (1)$$

where A and B are fit parameters. This expression is generally used to describe the high-temperature background [8]. The spectrum was then analyzed and the characteristics of the P1 peak, obtained with different compositions of single- and polycrystals, are summarized in Table 2. Figure 5 shows the Arrhenius plot obtained for the P1 peak in both single- and polycrystals.

TABLE 2—Recapitulation of characteristics of P1 peak.

Alloys	Condi- tions	T_p (K) at 1 Hz	Q^{-1} max ($\times 10^{-3}$)	τ_0 (sec)	Q (eV)	Peak Broad- ening α (%)	Self- Diffusion Energies [31]	
							Ni	Cr
Ni-20Cr single crystal	heating	949.7	...	4.3×10^{-17}	2.93	23	2.98	2.94
	cooling	949.5	...	5.0×10^{-17}	2.92	20.3
Polycrystal	heating	942.4	1.66	4.0×10^{-17}	2.92	18.2
Ni-33Cr single crystal	heating	997.6	...	2.7×10^{-17}	3.12	21.7
	cooling	1005.2	...	2.6×10^{-18}	3.35	...	3.07	3.02
Ni-31Cr polycrystal	heating	985.2	4.68	1.3×10^{-18}	3.35	33

In Ni-20Cr the activation energy is found to be 2.92 eV when the pre-exponential factor of the relaxation time τ_0 is of the order of 4×10^{-17} .

Possible Mechanism for the P1 Peak

Based on the experimental results shown in section "Experimental Results," it is reasonable to suggest that the P1 peak is related to a microscopic process taking place in the interior of the grains. Moreover, the activation energy of the associated process is found to be very close to the diffusion energies of nickel and chromium alloys (Table 2). Also, the peak is found to be 20 to 30% broader than a Debye peak. These values are reasonable for the point defect relaxation mechanisms. Figure 6 shows that the relaxation strength of the P1 peak depends strongly on the concentration c of chromium in the alloy and obeys approximately a $c^2(1 - c)^2$ relationship (Fig. 6). All these characteristics lead us to attribute the P1 peak to a Zener relaxation effect that is a stress-induced ordering phenomenon, which is a quite general property of substitutional solid solutions [8].

The detailed analysis of P1 peak can be found in Ref 23. It was shown that the characteristics of this peak can be well explained by the model of LeClaire and Lomer [29]. The relaxation mechanism of the P1 peak is then the consequence of stress-induced changes in the state of short-ranged order, since the lattice dimensions of the alloy depend upon the existing degree of both long- and short-ranged order. Thus the equilibrium degree in a strained state will in general differ from the one in the unstrained solid. The application of an applied shear stress then changes the equilibrium value of the order parameter in one direction relative to that in another direction. The rearrangement of atoms thereby produces anelastic relaxation [8,29].

It is important to mention that the interpretation of the P1 peak as a Zener relaxation is not absolutely certain. First, considering Fig. 4, it is clear that the P1 peak seems to have disappeared during cooling (curve 2a) even though the concentration of chromium has not changed. Second, measurements of Fig. 3 (see also Fig. 7) obtained in a single crystal show that the P1 peak appears at the beginning of an important increase of the background which is certainly correlated with some dislocation movement. Consequently it is possible that the P1 peak is due to dislocation dragging chromium atoms in substitutional solid solution [30]. In that case the disappearance of the peak during cooling is either correlated with some annealing of the

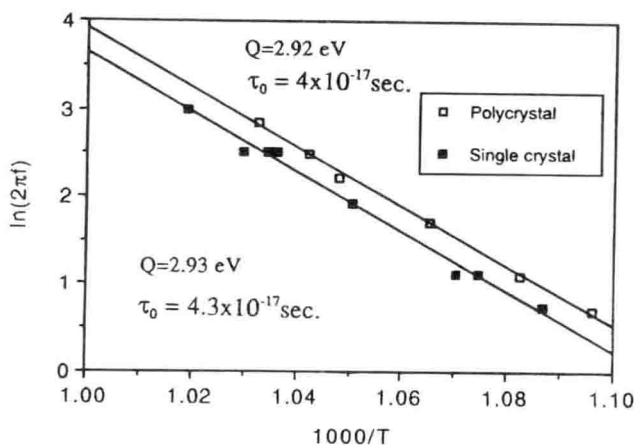


FIG. 5—Logarithm of frequency as function of P1 peak inverse temperature for single- and polycrystal Ni-Cr.